Blade-Tip Vortex Measurement by PIV

Atsushi MURASHIGE, Akihiko TSUCHIHASHI,
Tomoka TSUJIUCHI, Eiichi YAMAKAWA

Advanced Technology Institute of Commuter-helicopter, Ltd. (ATIC)

2 Kawasaki-Cho, Kakamigahara City, Gifu-Pref. 504, Japan

Abstract

For the basic understanding of the tip vortex structure during the blade-vortex interaction (BVI), the flow field measurement around the tip vortex of the rotating blade were made with the aid of 2-dimensional particle image velocimetry (PIV) system.

The measured data such as the flow field vectors, the core size and the circulation strength of the blade tip vortex are shown in this paper as the function of the rotor thrust level.

The results of the rotor noise measurement and the LLS flow visualization are also presented, which were performed in order to determine the test condition for the PIV measurement.

Notation

c	: Blade Chord Length
r	: Blade Spanwise Position
R	: Rotor Radius
Ω	: Rotor Rotational Speed
x/c,y/c,z/c	: Tip Vortex Position normalized by Blade Chord Length
α	: Shaft Angle of Model Rotor
U_∞	: Wind Tunnel Flow Velocity
Vtan	: Tangential Velocity of Vortex
μ	: Advance Ratio
Γ	: Circulation of Tip Vortex

1.Introduction

As the helicopter operations over populated city areas are increasing, the BVI noise during the approach flight is becoming the main problem of the helicopter external noise.

The BVI noise is generated by the rapid change of the blade surface pressure induced by the interaction of the tip vortices from the foregoing blades as shown in Fig.-1.

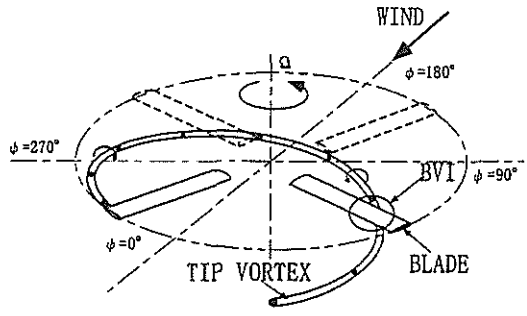

Figure-1 Concept of BVI Phenomenon

The analysis of this BVI noise is usually made through following 3 steps. (Ref.1)

step-1: Calculation of Rotor Wake Geometry and Circulation Strength by using Vortex Theory

step-2: Calculation of Blade Surface Pressure including BVI effect by using CFD

step-3: Calculation of Acoustic Field based on the Pressure Distribution obtained from step-2 by using Acoustic Equation

In order to increase the accuracy of the BVI noise analysis, more accurate calculation of the wake geometry and the vortex strength is required.

Therefore, it is very important to understand the position, the strength and the core radius of the tip vortex for this purpose.

To get these information, many researchers have studied the behavior of the blade tip vortex using the flow visualization techniques such as LLS (Laser Light Sheet), LDV(Laser Doppler Velocimetry) and so on. (Ref. 2,3)

Furthermore, the new flow measurement technique of PIV have been developed recently and already been applied to the flow around the rotor. (Ref.4)

This paper presents the PIV results performed by using a small model rotor of about 1m radius in order to get the information of the blade tip vortex.

The main objectives of this study are as follows.

(1)Acquisition of Basic Data of Blade Tip Vortex
(2)Acquisition of Validity Data for Wake Analysis
(3)Establishment of PIV Technique for the Rotor Flow Measurement

2.Test Apparatus

(1)Model Rotor Test Stand

For the PIV measurement of the blade tip vortex, the general model rotor test stand of Kawasaki Heavy Industries, Ltd. (KHI) was used. This test stand is designed for the general purpose of the helicopter wind tunnel tests such as the rotor performance test and the aerodynamic interference evaluation test between a rotor and a fuselage.

The drive motor of this test stand is a 37-HP electric magnetic motor controlled by an inverter system and has the capability to drive the small size model rotor of up to about 1.25m radius under the maximum rotational speed of 2400 rpm.

In order to measure the rotor forces and the fuselage forces, two sets of 6-force components internal balances are installed in this system and the outer fuselage shell is changeable according to the test purpose.

Because the fuselage aerodynamics is not so important in our study, a dummy fuselage shell of rotating NACA airfoil shape is applied and no fuselage forces are measured.

The hub is the 4-blades fully articulated type. The flapping angles can be measured by potentiometers and these signals are used for the trim control of the rotor.

The blade used in this test is the KHI's standard model blade made by composite material. The radius and the chord length of this blade are 961mm and 64.6mm respectively, and this blade has a linear twist of 10 degrees. The airfoil section is a combination of DKR120B (from root to 92%R) and DKR105B (at tip). The geometry of the tip region outer 92%R is a simple trapezoid (with taper ratio=0.6).

The picture is shown in Fig.-2 and the main feature of the test stand and the model rotor blade are shown in Table-1.

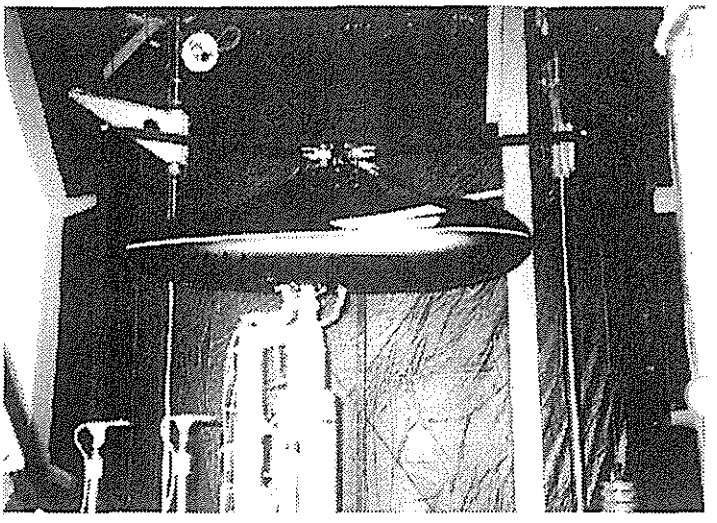

Figure-2 Picture of model rotor test stand

1	Rotor Test Stand	Motor Power	37HP max.
2		Hub Type	Fully Articulated
3		Balance	Rotor & Fuselage Balance
1	Model Blade	Rotor Radius	961mm
2		Chord Length	64.6mm
3		Twist	-10deg(linear)
4		Tip Shape	Trapezoid (>92%R)
5		Taper Ratio	0.6
6		Airfoil	DKR120B (root)
			DKR105B(tip)

Table-1 Main spec of model rotor test stand and model blade

(2)PIV System

In our PIV system, a double-pulse Nd-YAG laser of 400mJ maximum pulse energy is used to generate the laser light sheet.

The flow image data are obtained by the CCD camera of 2Kx2K pixels. Up to 10 image data can be taken in one time measurement process and these data are once stored into the hard disk unit before calculating the flow field data.

The basic hardware for the system control and the PIV processing is based on an IBM PC-AT compatible computer. This computer has two special interface cards in it. One is the timing control card to synchronize the laser emission with the CCD-camera shuttering and the rotating mirror speed, and the other is the digital signal processing card in

order to help a large amount of calculation in the PIV data processing.

The PIV software used in this test is on the market.

For the calculation of the velocity fields from the flow image data, we adopt the self-correlation algorithm. And we use the rotating mirror system in order to realize the image shift effect.

As the seeding particles, the vapor of propylene glycol is used and this vapor is injected into the flow through the seeding nozzle which is set upstream the honeycomb core for smoothing the wind tunnel air flow.

Table-2 shows the main feature of our PIV system.

1	Light Source	Double Pulse Nd-YAG Laser (maximum energy 400mJ)
2	Camera	2Kx2K Pixels CCD Camera
3	Measurement Area	300mmx300mm (max.) 150mmx150mm (usual)
4	Image Shift	Rotating Mirror Method
5	PIV Processing	DOS/V Computer with Timing Card and DSP Card
6	Software	VISIFLOW (AEA technology, Ltd.)
7	Seeding Particle	Vapor of Propylene Glycol

Table-2 Main spec of PIV system

3.Test Procedure

The model rotor and the PIV apparatus setup in the wind tunnel is shown in Fig.-3.

The wind tunnel used in this test is the 2.5m×2.5m low speed wind tunnel of Kawasaki Heavy Industries, Ltd. Its test section is open jet type and has an octagonal shaped jet nozzle. The model rotor system was mounted on the strut system and the rotor plane was about 200mm above the wind tunnel center line. Because the stiffness of the base plate to fix the strut system was unexpectedly soft, the maximum rotor speed in this test was restricted to about 900rpm in order to avoid the excessive vibration of the system.

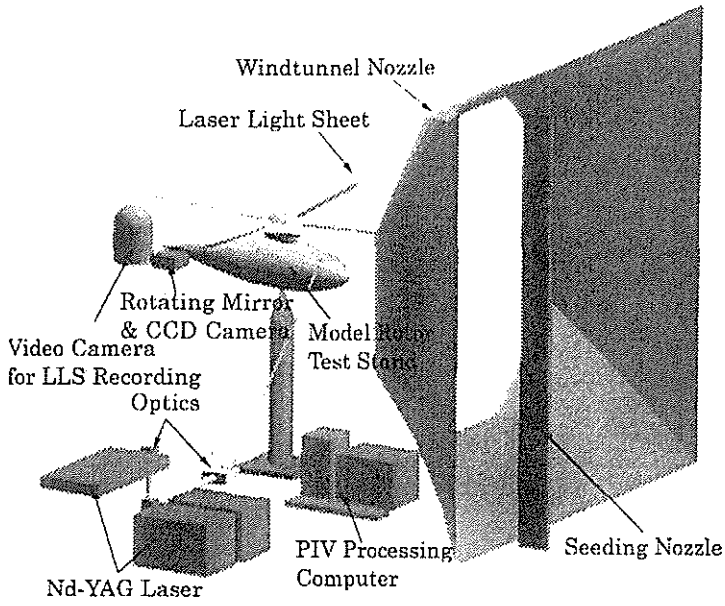

Figure-3 Setup of Model Rotor and PIV System

We made this PIV test by dividing the following 2 steps.

(1) Step 1 (noise measurement and LLS flow visualization)

In order to establish the test conditions of the PIV test, the rotor noise measurement and the LLS-flow visualization were performed prior to the PIV test.

For this purpose, the rotor operational conditions were changed parametrically as shown in Table-3.

1	Rotor RPM	600*1 and 881rpm
2	Advance Ratio	0.1~0.2 step 0.02
3	Rotor Shaft Angle	0~15deg step 2.5 deg
4	Rotor Thrust	CT=0.0058,0.0064,0.0070

*1:Only for LLS test

Table-3 Test conditions of acoustic and LLS tests

In the noise measurement test, the relationship between the rotor noise level and the flight condition was investigated with 3 microphones which were set at the positions of ψ=45°, 67.5°, 90°, r/R=80% and 1R below the rotor plane.(See Fig.-4)

These microphone positions were selected based on the CAMRAD wake analysis results to catch the BVI noise in the 1st quadrant of rotor plane. (From the CAMRAD results, the parallel BVI was expected at $\psi \fallingdotseq 60°$ under the flight condition of the middle range of advance ratio.)

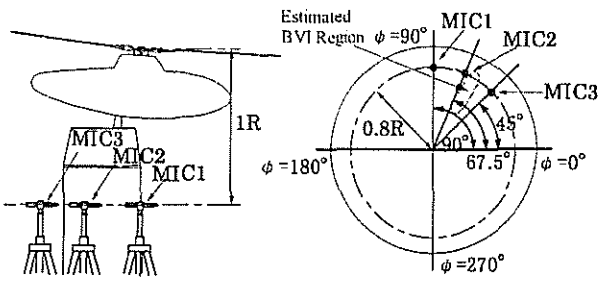

(a) side view (b) plan view

Figure-4 Microphone locations in the acoustic test

In the flow visualization test, the vortex images on 5 different planes (r/R=55%,65%,75%,85%,95% at ψ=50°) were recorded with the video camera in order to confirm the correlation between the noise level and the tip vortex position. (See Fig.-5)

The same laser light source and the same seeding particle were used as for the PIV measurement. To catch the image of the vortices passing under the blade, the flow field was illuminated from below the rotor plane.

In this flow visualization test, the rotor rotational speed was intentionally reduced to 600rpm in order to freeze the vortex image in the flow field by synchronizing the rotor rpm to the oscillating rate of the Nd-YAG pulse laser (=10Hz).

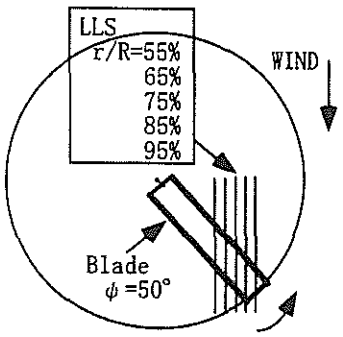

Figure-5 Flow visualization planes in the LLS test

(2) Step 2 (PIV measurement)

Based on the step 1 results, the maximum BVI noise condition (μ=0.16, α=7.5° and CT=0.0064) was selected as the nominal test condition of the PIV measurement. Only the rotor thrust level was changed parametrically around this nominal condition. (See Table-4)

1	Rotor RPM	881 rpm
2	Advance Ratio	0.16
3	Rotor Shaft Angle	7.5deg.
4	Rotor Thrust	CT=0.0058,0.0064,0.0070,0.0077

Table-4 Test conditions of PIV test

We selected 2 planes for the PIV measurement as shown in Fig.-6. One plane was selected near the blade tip at ψ =180° in order to get the vortex information just after the generation at the tip region. The other plane was near r/R=75% at ψ=50° . This plane was selected to acquire the vortex data in the advancing side BVI region.

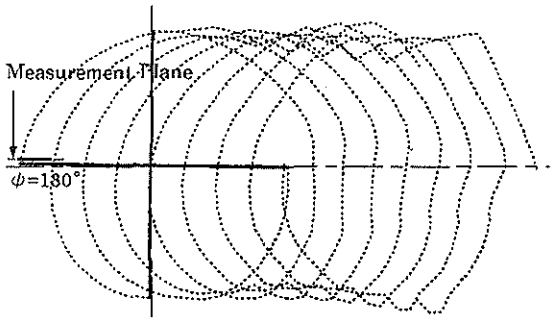

(a)Measurement plane for the tip vortex in the blade tip region

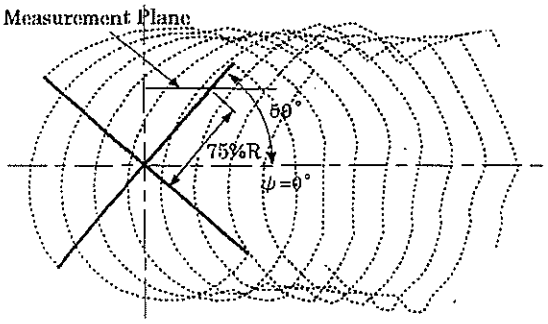

(b)Measurement plane for the tip vortex in the BVI region

Figure-6 Measurement planes in the PIV test

No synchronized measurement with the rotor rpm was performed in this PIV test, mainly because of the technical

problem of our measurement system.

The blade azimuth position could not be directly obtained for this reason, so the azimuth position was estimated from the tip vortex position on the CCD camera image based on the LLS flow visualization result and the CAMRAD calculation.

The rotor trim controls (collective and cyclic pitches) were adjusted so as to make the tip-path plane perpendicular to the rotor shaft for every test cases.

4.Results and Discussions

(1)Noise Measurement Result

Fig.-7 shows the influence of the flight condition on the rotor noise. The contour lines of this graph show the sound pressure levels measured at each advance ratio and shaft angle combination. All the noise data are subtracted by the wind tunnel background noise which was obtained in the no rotor cases. Because no correction was applied about the sound reflection effect at the wind tunnel wall, the absolute value of the sound pressure level of this result has no meanings. Only qualitative comparison is possible.

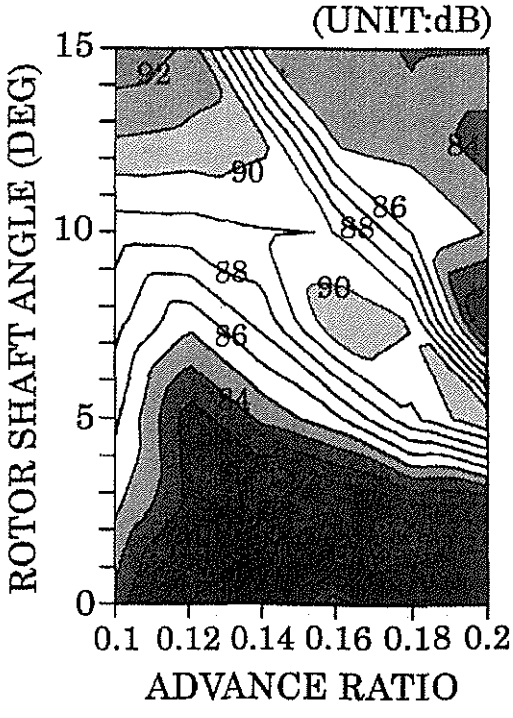

Figure-7 Contours of sound pressure level (dB) for the different flight conditions (microphone location = 67.5°)

From this figure, we can get the BVI occurrence condition as the ridge of the noise contours. In the middle range of the advance ratio where the helicopter usually uses during approach flight, we can see the maximum BVI noise will be generated under the condition around μ=0.16 and α =7.5° .

Fig.-8 shows the comparison of the maximum BVI noise condition between the experimental and the analytical results. The circle symbols are the experimental values which were obtained by extracting the noise peak condition from Fig.-7 and the solid line is the analytical value. The analytical value was obtained as the head-on BVI condition by using CAMRAD.

The agreement of the maximum noise condition of the test is fairly good with the head-on BVI condition in the CAMRAD analysis. From this fact, we can confirm the main part of the large noise generated in this test condition range is caused by the BVI phenomena.

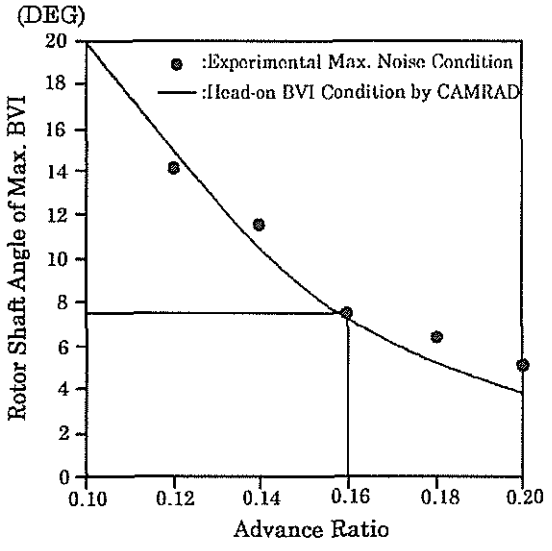

Figure-8 Comparison of the maximum BVI noise condition between the test and the analysis

(2)LLS Flow Visualization Result

Fig.-9 shows the tip vortex trajectories on X-Y plane (horizontal-plane) obtained by the LLS technique.

The solid lines with symbols are the LLS results and the dashed lines are the CAMRAD results.

As seen from this figure, there is a difference between the test and the analytical result concerning the X-positions of the vortices. This difference corresponds to about 5 degrees in azimuth angle. Except this azimuth difference, the flow

visualization result and the CAMRAD result show a good agreement in the wake trajectories and the interval length between each vortices.

Fig.-10 shows the tip vortex trajectories in the Y-constant plane (vertical-plane) which includes the blade section of ψ =50° and r/R=75%. The solid symbols are the LLS result and the open symbols are the CAMRAD result. In the CAMRAD result, the vortices' positions at 2 blade azimuth angles are shown for the correction of above mentioned 5 degrees azimuth difference of the wake geometry.

By shifting the azimuth angle, the vertical positions of the tip vortices calculated by CAMRAD also shows the good agreement with the experimental result.

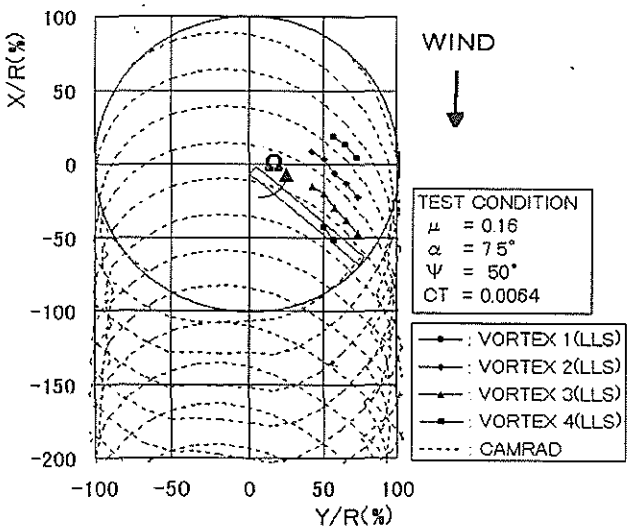

Figure-9 Plan view of the tip vortex trajectories obtained by LLS visualization

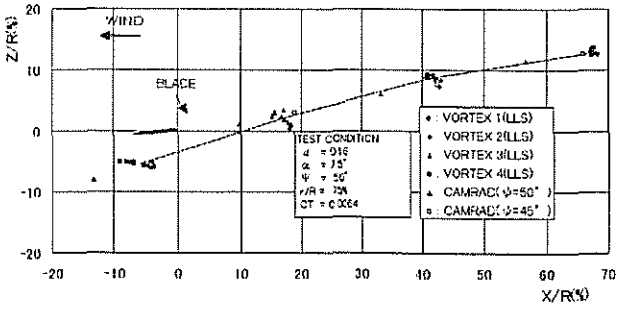

Figure-10 Side view of the tip vortex trajectories obtained by LLS visualization

From the acoustic test and the LLS visualization test, we can get the correlation between the rotor noise level and the tip vortex position with the help of CAMRAD analysis.

(3)PIV Measurement Result

The condition of μ=0.16, α=7.5° and CT=0.0064 was obtained as the maximum BVI condition in the middle range of the flight speed from the acoustic test. Therefore, we selected this condition as the nominal test condition for the PIV measurement.

Fig.-11 shows the velocity vectors in the flow field of the blade tip region at $\psi \fallingdotseq 180°$ measured by the PIV system.

In this figure, all the velocity vectors were subtracted by the velocity of the vortex center in order to make the flow rotation around the tip vortex clearer.

From this figure, we can see that the tip vortex is generated at the slightly inboard position of the blade tip region (about 97%R). The vortex at this region has a very flat shape because it is still in the very beginning stage of tip vortex roll-up process. The vortex core size obtained from the velocity profile along the vertical line is about 18% c.

This value is somewhat lager than the result of Ref. 4. (about 10% c in mean core size) The main reason of this difference is probably caused from the difference of the tip shapes between our test and Ref. 4. (trapezoid and rectangle)

In this figure, the averaged velocity data of 20 images are also shown. By taking average, the scattering of the velocity field is well smoothed. But the magnitude of the peak velocity vector becomes dull and the small profile of the flow field disappears.

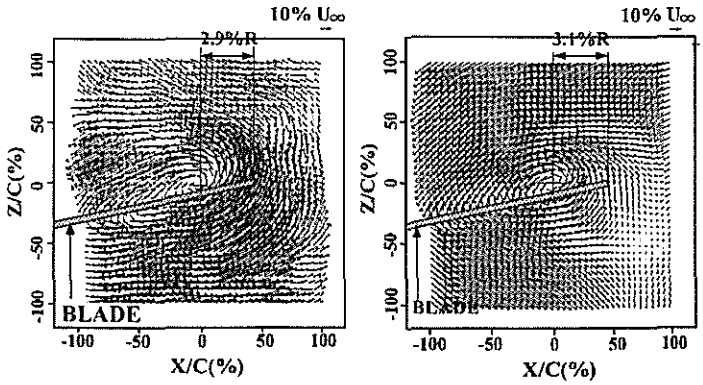

(a)Velocity vectors calculated from single image

(b)Averaged velocity vectors calculated from multiple images

Figure-11 Flow field in the tip vortex generation region at $\psi \fallingdotseq 180°$
(test condition: μ=0.16, α=7.5° ,CT=0.0064)

Fig.-12 shows the velocity vectors in the BVI region at $\psi \fallingdotseq 50^\circ$. The same data processing as at $\psi \fallingdotseq 180^\circ$ was applied to this data.

From this figure, we can see that the vortex is fully developed and its shape has nearly circle in this region.

And the increase of the tangential velocity magnitude around the vortex according to the rotor thrust level can be seen in this figure.

By taking average of multiple image data, the reduction of the peak velocity magnitude occurs again.

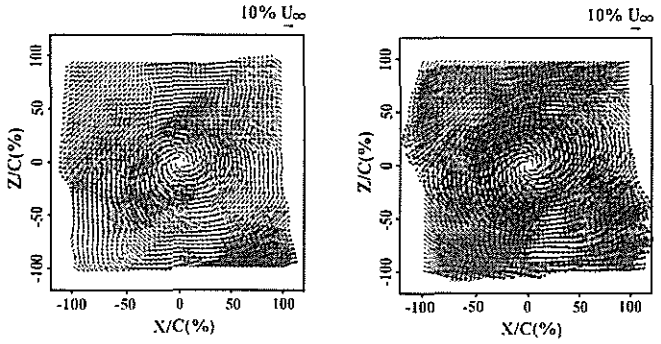

(1)CT=0.0064 (2)CT=0.0077

(a)Velocity vectors calculated from single image

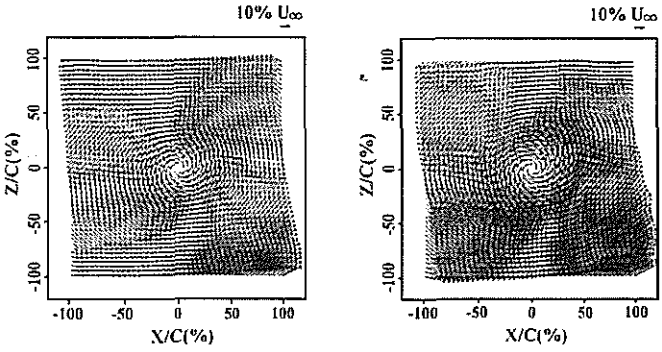

(1)CT=0.0064 (2)CT=0.0077

(b)Velocity vectors calculated from multiple images

Figure-12 Flow field in the BVI region at $\psi \fallingdotseq 50^\circ$
(test condition: μ=0.16, α=7.5°)

Fig.-13 shows the tangential velocity dustribution along the vertical centerline of the tip vortex. The individual velocity distributions from 8 measurements and the averaged velocity distribution are presented. Because the tip vortex trajectory intersected obliquely with the laser light sheet of the PIV in this region, the tangential velocity data were corrected with the following formula.

Vtan(corrected)=Vtan(measured) / cos(intersect angle)

The velocity distribution in the tip vortex core can be obtained in this figure.

By comparing the velocity distributions of 8 individual measurement results, we can see that there is about 30% maximum fluctuation of velocity among each results. This is probably due to the individual differences among 4 blades, since the measured data contains the vortex information from all 4 blades because of the non-synchronized measurement with the rotor rpm.

This fluctuation among each measurements makes the averaged velocity profile dull as shown in Fig.-13(b).

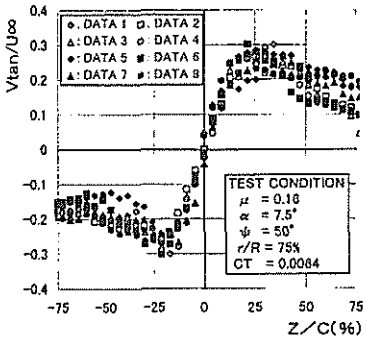

(a)Velocity distribution obtained from single image

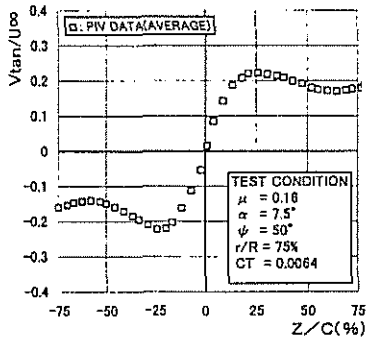

(b)Averaged velocity distribution obtained from multiple images

Figure-13 Tangential velocity distribution of the TIP vortex in the BVI region at $\psi \fallingdotseq 50^\circ$
(test condition: μ=0.16, α=7.5° ,CT=0.0064)

Fig.-14 shows the relationship between the mean vortex core size and the rotor thrust level obtained from the vortex data in the BVI region. From this figure, we can see that the core radius remains about 25% c at each rotor thrust levels.

The dependency of the core size on the rotor thrust level is not so clear, but we can see the tendency that the core radius increases slightly according to the thrust level.

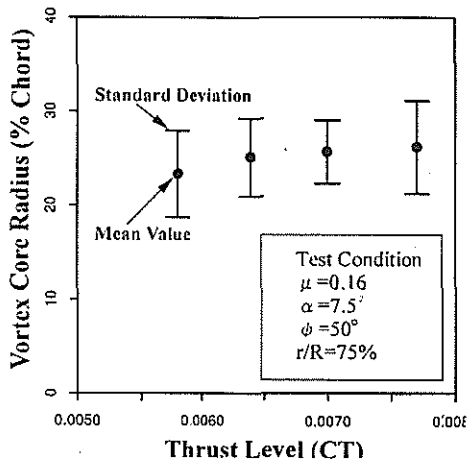

Figure-14 Relationship between the tip vortex core radius

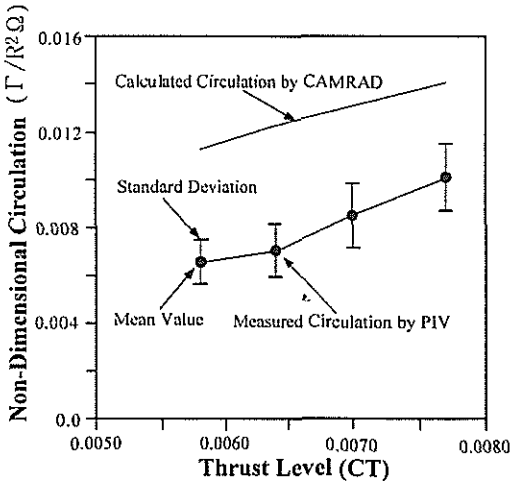

Figure-15 Relationship between the BVI vortex circulation and the rotor thrust

Fig.-15 shows the mean circulation of the BVI vortex related to the rotor thrust level.

To deduce the circulation value from the experimental data, we assumed the Scully model of the velocity distribution in the vortex core and get the vortex circulation strength as the Scully model's parameter by using the curve-fitting technique.

The circle symbols are the experimental circulation values and the solid line is the CAMRAD result.

As shown in this figure, both values increase proportionally to the rotor thrust level.

But the experimental circulation shows about 30~40% lower value than the CAMRAD result.

One reason of this difference is due to the dissipation of the vortex by the viscosity effect while the vortex passes through the flow field during the period of about 1.5 rotor revolutions. The other reason is probably because the CAMRAD analysis can't treat correctly the effect of the trapezoidal tip shape on the tip vortex.

In order to confirm these reasons, we are thinking about an additional PIV test in near future, in which the vortex data for the difference azimuth angles and the different tip shapes will be measured. And we also would like to try the further study about the blade tip vortex by using another measurement technique or CFD.

5.Conclusion

From this PIV testing, we conclude as follows.

(1)The PIV measurement of the instantaneous flow field around the tip vortex was performed successfully.

(2)The core size and the circulation strength of the tip vortex in the BVI region were obtained as a function of rotor thrust level.

(3)Averaging technique by use of multiple images supplies the very well smoothed flow field results but has a risk to miss the small flow structures.

References

1. T.Aoyama, N.Kondo, M.Aoki, H.Nakamura, S.Saito, "Calculation of Rotor Blade-Vortex Interaction Noise", 22nd European Rotorcraft Forum, Brighton, UK, Sept., 1996.
2. E.Mercker, K.Pengel, "Flow Visualization of Helicopter Blade Tip Vortices - A quantitative technique to determine the trajectory and the position of tip vortex pattern of a model rotor", 18th European Rotorcraft Forum, Avignon, France, Sept., 1992
3. S.A.Gorton, D.R.Polling, L.Dadone, "Laser Velocimetry and Blade Pressure Measurements of a Blade-Vortex Interaction", the American Helicopter Society 49th Annual Forum, St. Louis, Missouri, May, 1993.
4. U.Seelhorst, M.Raffel, C.Willert, H.Vollmers, K.A.Büterfisch, J.Kompenhans, "Comparision of Vortical Structures of a Helicopter Rotor Model Measured by LDV and PIV", 22nd European Rotorcraft Forum, Brighton, UK, Sept., 1996.